Organic Electronics 118 (2023) 106798

Contents lists available at ScienceDirect

Organic Electronics

journal homepage: www.elsevier.com/locate/orgel

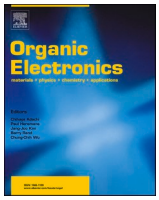

Hole versus electron transport in fullerenes☆

Eunkyung Cho, Veaceslav Coropceanu **, Jean-Luc Brédas *

Department of Chemistry and Biochemistry, The University of Arizona, Tucson, AZ, United States

A B S T R A C T

We have carried out density functional theory (DFT) calculations to derive the microscopic parameters that describe the hole and electron transport properties in C_{60} and C_{70} and their derivatives. The computed relaxation energies and the results of normal-mode analyses point out that there are no significant differences between the electron-vibration couplings and hole-vibration couplings in the C_{60} systems, where the differences between the reorganization energies for hole and electron transfers do not exceed 10 meV, except in the case of the parent C_{60} system where this difference is about 40 meV. The DFT estimates of the electronic couplings for holes and electrons in C_{60} and its derivatives are also found to be very similar. Thus, our theoretical results confirm the conclusions of recent experimental investigations that underline that the C_{60} fullerenes should not be regarded as just n-type transporting materials but in fact are intrinsically ambipolar. The DFT calculations performed for C_{70} show that the reorganization energy for hole transport is slightly lower (5 meV) than for electron transport and this difference is even larger, up to 100 meV, in the functionalized C_{70} systems. These results suggest that hole mobilities in C_{70} and its derivatives could also be comparable or even larger than the corresponding electron mobilities. In addition, the DFT calculations indicate that, with respect to unsubstituted fullerenes, the derivatization has a much larger impact on the ionization potential energies than on the electron affinity energies, which are both reduces; therefore, chemical modifications could be further exploited to decrease the intrinsically high IP values of C_{60} and C_{70} and lead to a better match with the workfunctions of common electrodes, which would facilitate hole injection.

1. Introduction

The C_{60} and C_{70} buckminsterfullerenes have led to a remarkable revolution in a broad range of applications including solar cells, hydrogen gas storage, or biomedical devices due to their redox properties, stability induced by their high symmetry, and strong electron accepting ability related to sp^2-hybridized carbons [1–7]. Also, fullerene derivatives carrying various functional groups have been exploited in organic electronics. For instance, derivatives such as [6,6]-phenyl--C_{61}-butyric acid methyl ester ([60]-PCBM) [8], [6,6]-phenyl-C_{71}-butyric acid methyl ester ([70]-PCBM) [9], and indene-C_{60} bis-adduct ([60]-ICBA) [10,11] have received great attention in the field of organic photovoltaics [10–19]. There is also a major interest in using fullerenes and fullerenes derivatives as active materials for applications in field-effect transistors and photodetectors [20].

In context of organic electronics, the fullerenes and their derivatives are principally used as electron accepting and electron transporting materials. However, it was also demonstrated that they could be exploited as electron donor materials in organic solar cells [21–23]. Their characteristics as hole transporters were addressed in several instances [24–27]. For example, it was found that solution-processed [60]-PCBM displays ambipolar transport properties with equivalent hole and electron mobilities of about $\sim 10^{-3}$ cm^2 V^{-1} s^{-1} [24]. It was also reported that the bulk hole mobility of [60]-ICBA is high and equivalent to its bulk electron mobility, *ca.* 3×10^{-3} cm^2 V^{-1} s^{-1} [25]. In a recent study, Wetzelaer and Blom concluded that fullerenes should not be regarded as just n-type transporting materials since they are intrinsically ambipolar [27].

In order to shed more light on the charge-transport properties of the fullerenes, we carried out density functional theory (DFT) calculations to derive the main microscopic parameters, *i.e.,* the transfer integrals and vibrational couplings, that determine hole and electron transport. We considered two types of fullerenes, C_{60} and C_{70}, and their derivatives: the PCBM mono- and bis-adducts, *i.e.*, [60]-PCBM, [70]-PCBM, [60]-bis-PCBM, and [70]-bis-PCBM, as well as the mono-, bis-, and tri-indene adducts of C_{60}, *i.e.*, [60]-ICMA; [60]-ICBA and [60]-ICBA-2; and [60]-ICTA (see Fig. 1).

☆ This work is dedicated to the memory of Professor Martin Pope, a pioneer and giant of the field of organic electronics, and a mentor who inspired generations of scientists.

* Corresponding author.
** Corresponding author.
E-mail addresses: coropceanu@arizona.edu (V. Coropceanu), jlbredas@arizona.edu (J.-L. Brédas).

https://doi.org/10.1016/j.orgel.2023.106798
Received 7 February 2023; Accepted 17 March 2023
Available online 23 March 2023

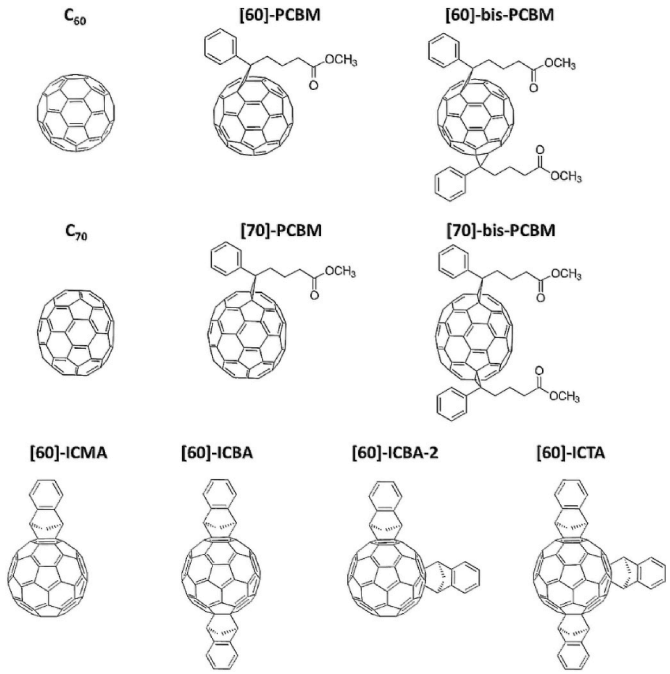

Fig. 1. Chemical structures of C_{60}, C_{70}, and their derivatives investigated in this work.

2. Computational methodology

Density functional theory (DFT) calculations were carried out at the B3LYP/6-31G (d,p) level with the Gaussian 16 package [28] to determine the geometrical and charge-transfer properties of C_{60}, C_{70}, and their derivatives. Geometry optimizations of the molecules in their neutral and charged (radical-anion and radical-cation) states were performed. The intramolecular reorganization energies were determined via examination of the potential energy surfaces for the neutral and charged states [29] as well as via normal-mode analysis. We used the DUSHIN program [30] to perform the decomposition into the contributions of each normal mode to the total relaxation energy of the molecules and to determine the electron-vibration couplings and Duschinsky matrices. The evaluations of the hole and electron transfer integrals were based on the crystal structures and were derived via a fragment orbital approach in combination with a basis set orthogonalization procedure [31,32], based on the B3LYP/6-31G (d,p) results. The rate constants for hole and electron transfers were estimated using the semiclassical Marcus theory [33].

$$k_{hole(electron)} = \frac{2\pi}{\hbar} t_{h(e)}^2 \frac{1}{\sqrt{4\pi\lambda_{h(e)} k_B T}} exp\left[-\frac{\left(\lambda_{h(e)} + \Delta G\right)^2}{4\lambda_{h(e)} k_B T} \right] \quad (1)$$

Here, $\hbar$, k_B, T, $\lambda_{h(e)}$, $t_{h(e)}$, and ΔG denote the reduced Planck constant, Boltzmann constant, temperature, reorganization energy, hole (or electron) transfer integral, and site free-energy difference, respectively. When the highest occupied molecular orbitals (HOMOs) and the lowest unoccupied molecular orbitals (LUMOs) are degenerate, the hole (or electron) transfer integrals were calculated by accounting for the exact degeneracy of the molecular orbitals, as discussed in our earlier work [34]:

$$t_{h(e)}^2 = \frac{1}{g_a} \sum_{ij} \left(\Psi_{ai} | H | \Psi_{bj} \right)^2 \quad (2)$$

where g_a is the degeneracy of the Ψ_{ai} and Ψ_{bj} orbitals on molecules a and b.

3. Results and discussion

3.1. Redox properties

The highly symmetric C_{60} molecule (I_h point group) [35] has only two types of bonds: a double-like bond connecting two hexagonal rings and a single-like bond connecting one pentagonal and one hexagonal ring. The bond lengths in the optimized neutral C_{60} are 1.396 Å for the double bond and 1.453 Å for the single bond. Due to their high molecular symmetry, the energy levels of C_{60} can show high orbital degeneracy; for instance, the LUMO level is three-fold degenerate while the HOMO level is five-fold degenerate (see Fig. 2).

Upon addition of one electron to the three-fold degenerate LUMO level of C_{60}, the symmetry of the stable geometric configurations of the resulting anion-radical state is lowered to D_{5d}, D_{3d}, or D_{2h} as a result of Jahn-Teller distortions [36–38]. The lengths of the single bonds are no longer equivalent and deviate from the original bond lengths in neutral C_{60}; the same is true for the double bonds. As a result, the size of the fullerene cage slightly changes when an electron is added (see Fig. S1) [39]. Similar effects take place upon oxidation of C_{60} [38,40].

The C_{70} molecule belongs to the D_{5h} symmetry point group and has eight inequivalent bonds [41]. Upon reduction and oxidation, according to our DFT calculations, the C_{70} cage also slightly varies [42]. Mono- and bis-substituted PCBM molecules based on C_{60} and C_{70} and mono-, bis-, and tri-indene adducts of C_{60} also show changes in cage size upon addition or removal of an electron; these geometrical changes are related to the relaxation energies described below.

We first discuss the computed electron affinity (EA) values of the investigated molecules, which are collected in Table 1. For the sake of comparison, the DFT values of the HOMO and LUMO levels are given in Table S1. As seen from Table 1, the EA of C_{60} is slightly lower (~0.1 eV) than that of C_{70}, which is in line with experimental data [43–47]. Introduction of the mono-, bis-, and tri-indene functional groups on the fullerenes leads to a decrease of EA values by around 0.1 eV per number of substitutions. Also, the electron affinity decreases upon going from C_{60} or C_{70} to the corresponding PCBM and bis-PCBM. These reductions in the EA values upon attaching and increasing the number of functional groups are also consistent with experimental results [10,48–51].

We now turn to the ionization potentials (IPs). The IP of C_{60} is

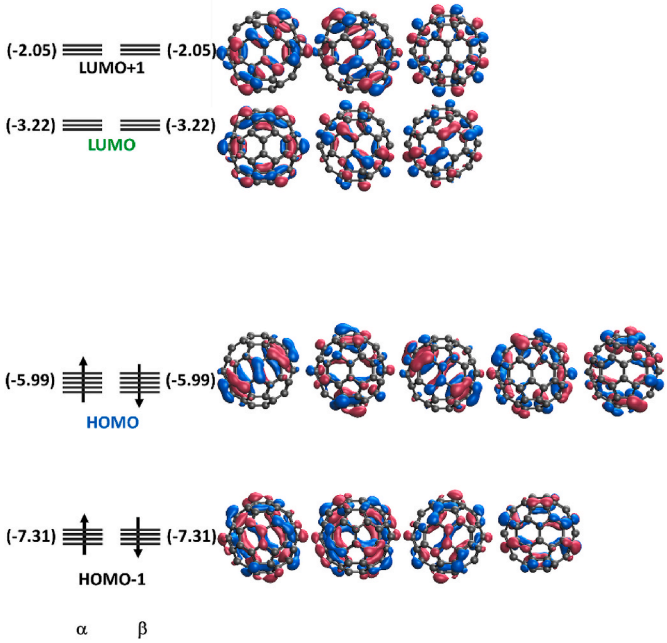

Fig. 2. Energies (in eV) and wavefunctions of the frontier molecular orbitals of neutral C_{60}, as obtained at the B3LYP/6-31G (d,p) level of theory.

Table 1
Vertical and adiabatic electron affinities (EAs) and ionization potentials (IPs) for C_{60} and C_{70}, and their derivatives, as calculated at the B3LYP/6-31G (d,p) level of theory. All values are given in eV.

Molecule	VEA	AEA	VIP	AIP
C_{60}	2.00	2.06	7.23	7.14
[60]-PCBM	1.92	2.00	6.82	6.74
[60]-bis-PCBM	1.86	1.94	6.55	6.47
[60]-ICMA	1.89	1.96	6.78	6.72
[60]-ICBA	1.80	1.87	6.50	6.43
[60]-ICBA-2	1.72	1.79	6.54	6.47
[60]-ICTA	1.65	1.72	6.31	6.24
C_{70}	2.08	2.15	7.10	7.02
[70]-PCBM	1.97	2.06	6.69	6.63
[70]-bis-PCBM	1.87	1.98	6.37	6.31

slightly higher than that of C_{70}, which is consistent with the reported experimental data [52,53]. Upon introducing functional groups, the IP value decreases continuously with their number [52–54]. These results imply that the functionalized fullerenes can more easily donate electrons compared to C_{60} and C_{70}. Overall, as seen from Table 1, the functionalization of C_{60} and C_{70} has a much larger effect on the molecular IP than on the EA. Indeed, in both C_{60} and C_{70} series, the EA values vary by at most 0.35 eV, while the IP values vary by over 0.9 eV.

It is important to note that the present calculations do not include the effect on the EA and IP values of the electronic polarization due to a solid-state environment (this effect can in each case exceed 1 eV) [55]. The experimental IP values of C_{60} and C_{70} in the solid state are 6.17 eV and 6.35 eV, respectively [55–57]. These values are significantly larger than the workfunctions (about 5 eV) of the anodes that are typically used in organic electronic devices [58]. The consequence is very large injections barriers for holes in the case of fullerene semiconductors, which appears to be the main reason why hole transport in fullerenes is challenging to observe [27]. For the sake of comparison, we note that the IP of pentacene, one of the prominent hole-transporting materials, is about 5 eV [59]. From Table 1, among the series of fullerenes we considered, [60]-ICBA and [60]-ICTA are expected to exhibit the lowest hole injection barriers when considering conventional anodes such as indium-tin oxide.

3.2. Relaxation energies

We recall that, in charge transport theory, the electron (hole)-vibrational couplings and related reorganization energies represent a major set of microscopic parameters [29]. According to Marcus theory, a lower reorganization energy leads to a lower hopping barrier for charge transfer, see Eq. (1). The calculated relaxation energies and the associated reorganization energies [29] for C_{60}, C_{70}, and their derivatives, corresponding to the geometrical changes between neutral and charged molecules related to an electron or a hole transfer event, are listed in Tables 2 and 3, respectively. The results obtained from adiabatic-potential-surface (AES) analyses and normal-mode (NM) analyses are in very good mutual agreement. In the case of electron transport, the estimated reorganization energy of C_{60}, 0.135 eV (see Table 2), is consistent with the results of previous calculations, 0.132 eV [60] and 0.140 eV [61]. Upon adding one or two phenyl butyric acid methyl ester functional groups to C_{60}, the reorganization energy increases in each case by some 10 meV. The reorganization energies of [60]-ICMA and [60]-ICBA are very close to that of C_{60} and slightly smaller than in [60]-PCBM. The largest reorganization energies among the C_{60} derivatives are found for [60]-ICBA-2 and [60]-ICTA. On the other hand, the reorganization energy of the C_{70}-based molecules increases by ~35 meV every time a PCBM functional group is added. Overall, in the case of electron transfer, the reorganization energies of C_{70} and its derivatives are larger than in the related C_{60} molecules.

Interestingly, the reorganization energies for holes (see Table 3) decrease when adding functional groups to the fullerenes, which is opposite to the trend observed for electrons. For instance, the λ_h value for C_{60} is estimated to be about 178 meV, while for [60]-ICBA it reduces to 135 meV. Also, the reorganization energies estimated for hole transport in C_{70} and its derivatives are smaller than in the corresponding C_{60} molecules.

The decomposition of the relaxation energies into the contributions from the normal modes is shown in Fig. 3 for C_{60} and C_{70} and in Figs. S2–S4 for the other molecules. The results of the normal-mode calculations indicate that, in the case of electron transport, the relaxation energies in C_{60} mainly arise from high-frequency vibrations (1400-1600 cm^{-1}); the largest contributions come from modes at 1472 cm^{-1} (21%), corresponding to a symmetric C=C stretching mode, 1425 cm^{-1} (21%), and 1584 cm^{-1} (18%). These results are consistent with previous studies on C_{60} [62–64] indicating that the large electron-vibrational couplings are due to H_g modes. In the case of hole transport, both high-frequency and low-frequency (200-400 cm^{-1}) vibrations participate in the reorganization energy, with the largest contributions coming from modes at 261 cm^{-1} (42%), 1425 cm^{-1} (19%), and 1584 cm^{-1} (15%). When going from C_{60} to [60]-bis-PCBM, the contribution of low-energy modes to the reorganization energy increases in the case of electrons while it decreases for holes. In the C_{70} derivatives, normal modes in two distinct ranges, 200-800 cm^{-1} and 1000-1600 cm^{-1}, contribute to the relaxation energies of both holes and electrons.

The comparison of the values listed in Tables 2 and 3 indicates that, for C_{60}, the reorganization energy for hole transport is about 40 meV larger than in the case of electron transport. According to the normal-mode analyses, this difference is due to large contributions from low-frequency modes in the case of hole transfer. In the C_{60} derivatives, the reorganization energies for holes are also larger than for electron transport; however, the related energy differences do not exceed 10

Table 2
Relaxation energies (in meV) for the neutral state and anion state, λ_N and, λ_A, and reorganization energies, λ_e, in C_{60} and C_{70}, and their derivatives, as computed using the adiabatic potential surfaces of both neutral and anion states and normal-mode analyses.

Molecule	Adiabatic potential surface			Normal-mode analysis		
	λ_N	λ_A	λ_e	λ_N	λ_A	λ_e
C_{60}	70	65	135	68	67	135
[60]-PCBM	72	72	144	73	72	145
[60]-bis-PCBM	79	80	159	80	82	162
[60]-ICMA	69	68	137	69	68	127
[60]-ICBA	69	69	138	70	69	139
[60]-ICBA-2	75	74	149	75	74	149
[60]-ICTA	75	74	149	75	74	149
C_{70}	80	67	147	80	77	157
[70]-PCBM	95	90	185	95	94	189
[70]-bis-PCBM	105	116	221	106	105	211

Table 3
Relaxation energies (in meV) for the neutral state and cation state, λ_N and λ_C, and reorganization energies, λ_h, in C_{60}, C_{70}, and their derivatives, as computed using the adiabatic potential surfaces of both neutral and cation states and normal-mode analysis.

Molecule	Adiabatic potential surface			Normal-mode analysis		
	λ_N	λ_C	λ_h	λ_N	λ_C	λ_h
C_{60}	90	88	178	88	88	176
[60]-PCBM	76	74	150	76	75	151
[60]-bis-PCBM	76	74	150	76	74	150
[60]-ICMA	71	69	140	71	69	140
[60]-ICBA	68	67	135	68	67	135
[60]-ICBA-2	73	71	144	73	71	144
[60]-ICTA	76	74	150	77	75	152
C_{70}	62	80	142	63	60	123
[70]-PCBM	59	59	118	59	60	119
[70]-bis-PCBM	61	61	122	60	62	122

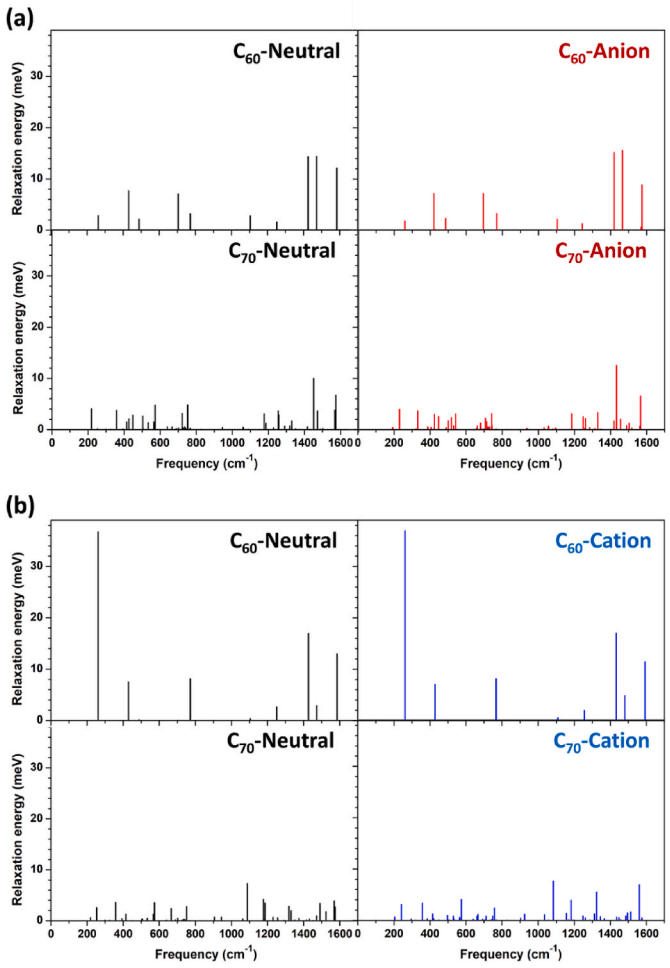

Fig. 3. Individual contributions of the normal modes of C_{60} and C_{70} to the relaxation energies (a) in the case of electron transport and (b) in the case of hole transport.

meV. In the case of C_{70}, the reorganization energy for hole transfer is slightly smaller (5 meV) than that for electron transfer; however, this difference increases up to 100 meV in the [70]-PCBM and [70]-bis-PCBM.

Finally, it is important to bear in mind that, according to our previous investigations [65,66] the chemical functionalization of the fullerenes can significantly increase the static disorder in the material. Such an increase in disorder would be detrimental to the charge-transport properties [29].

3.3. Electronic couplings

We focus now on a discussion of the transfer integrals, *i.e.*, electronic couplings. The transfer integrals are the second major set of microscopic parameters (in addition to the electron (hole)-vibrational couplings) that define the charge-transport properties [29]. To compute these couplings, the knowledge of the geometry configurations of the pairs of molecules involved in an electron (hole) transfer event is needed. Here, our calculations are based on the experimental crystal structures. Since only the crystal structures of C_{60} [67], [60]-PCBM [68], and [60]-ICBA [69] are available, the results discussed below are limited to these three systems (see Fig. 4).

As mentioned above, the frontier molecular orbitals of the systems we study here can be several-fold degenerate, leading to multiple transfer integrals describing charge transfer in the related molecular pairs. Therefore, for the sake of clarity, we report in Table 4 a single effective transfer integral computed in the way described in the Methodology section. As seen from Table 4, the largest values of the transfer integrals computed for electron transfer in C_{60}, [60]-PCBM, and [60]-ICBA are comparable and in the range of 15–26 meV. The same trend is observed for the transfer integrals describing hole transport, which are in the range of 20–31 meV. Overall, the DFT results point to transfer integrals for holes and electrons in C_{60}, [60]-PCBM, and [60]-ICBA as having comparable values. These results, taken together in Eq. (1) with those derived for the reorganization energies, yield comparable hole and electron transfer rate constants, see Table 5.

Lastly, we note that, while the crystal structures for the C_{70} materials are unavailable and therefore we did not provide estimates for the transfer integrals in these systems, field-effect transistor measurements have shown that the electron mobilities in C_{70} and [70]-PCBM are comparable to the values measured for their corresponding C_{60}-fullerene counterparts [70]. These results strongly suggest that the electronic couplings for electrons in the C_{70}-fullerene crystals should be similar to the values listed in Table 4 for the C_{60} systems.

4. Conclusions

The charge-transfer properties of the C_{60} and C_{70} fullerenes and their PCBM and indene derivatives, have been evaluated at the density functional theory level. Our results show that the adducts have a much larger effect on the IP energy than on the EA energy of the substituted

Table 4
Transfer integrals (in meV) for holes and electrons, as calculated for the pairs of molecules shown in the unit cells of Fig. 4.

	C_{60}		[60]-PCBM		[60]-ICBA-2	
	t_h	t_e	t_h	t_e	t_h	t_e
Pair 1	20.1	25.6	23.4	2.32	28.0	14.6
Pair 2	17.9	22.8	2.49	0.36	4.20	0.49
Pair 3	20.2	22.0	1.22	0.68	29.2	6.10
Pair 4			31.0	24.4	13.4	12.4
Pair 5			6.36	1.45	7.80	7.27
Pair 6					0.19	1.39
Pair 7					28.0	14.6

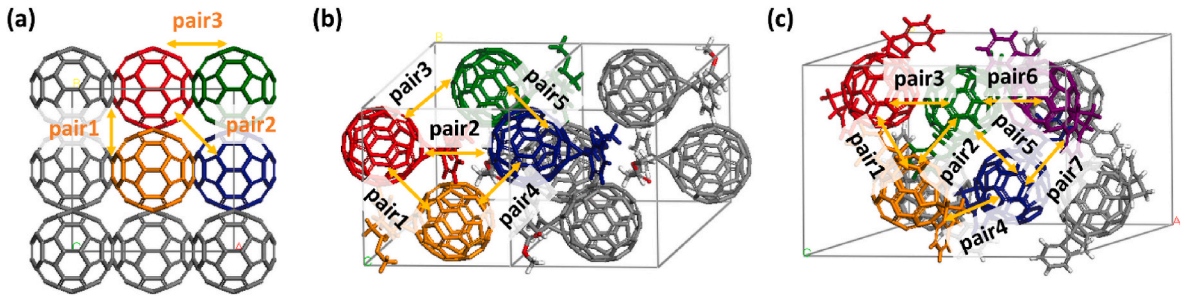

Fig. 4. Illustration of the molecular pairs in the crystals of (a) C_{60}, (b) [60]-PCBM, and (c) [60]-ICBA-2, considered for the calculations of the transfer integrals.

Table 5
Rate constants (in s^{-1}) calculated for hole transfer (k_h) and electron transfer (k_e), using the largest transfer integrals in C_{60}, [60]-PCBM, and [60]-ICBA-2.

	C_{60}	[60]-PCBM	[60]-ICBA-2
$\log k_h$	12.5	13.0	13.0
$\log k_e$	12.9	12.8	12.4

fullerenes. For example, when going from C_{60} to ICTA, the IP value decreases by about 0.9 eV. Thus, chemical modifications could be further exploited to reduce the intrinsically high IP values of C_{60} and C_{70} and better match the workfunctions of common electrodes.

Our calculations indicate that the reorganization energies for hole transport in the C_{60} derivatives are larger than those for electron transfer. C_{70} has smaller hole relaxation energies compared to C_{60} and substitution leads to even smaller relaxation energies; the opposite trend is obtained in the case of reduction. The results of normal-mode analyses characterize the hole-related relaxation energies of C_{60} and its derivatives as mainly due to high-energy vibrations (1400-1600 cm^{-1}); in C_{70} and its derivatives, modes in both the 200-800 cm^{-1} and 1000-1600 cm^{-1} ranges contribute to the reorganization energies. In the case of electron transport, low-energy and high-energy modes both participate in the reorganization energies of C_{60} and C_{70}. Overall, our calculations point out that, in most of the investigated systems, there are no major differences between the electron-vibration couplings and hole-vibrational couplings since the related differences between reorganization energies for holes and electrons do not exceed 10 meV. The exceptions are C_{60}, [70]-PCBM, and [70]-bis-PCBM, where the differences between reorganization energies increase to *ca.* 40, 70, and 100 meV, respectively.

We also estimated the transfer integrals for both hole transport and electron transport in C_{60}, [60]-PCBM, and [60]-ICBA. As for the vibrational couplings, the DFT estimates of the transfer integrals for holes and electrons are similar. Thus, our theoretical results confirm the conclusions of recent experimental investigations [27] that charge transport at least in the C_{60} fullerenes is intrinsically ambipolar. While additional investigations would be welcome to provide for the fullerene systems a more comprehensive understanding of the charge-transport properties and of the ways to better control them, we hope that the recognition by the organic electronics community that fullerenes can conduct holes as effectively as electrons will lead to new applications of these fascinating materials.

Declaration of competing interest

The authors declare that they have no known competing financial interests or personal relationships that could have appeared to influence the work reported in this paper.

Data availability

Data will be made available on request.

Acknowledgments

This work was supported by the National Science Foundation and the Air Force Research Laboratory through DMREF-2118578 and by the College of Science of the University of Arizona. The authors are thankful for the use of the High Performance Computing (HPC) resources supported by the University of Arizona TRIF, UITS, and Research, Innovation, and Impact (RII) Offices and maintained by the Research Technologies Department.

Appendix A. Supplementary data

Supplementary data to this article can be found online at https://doi.org/10.1016/j.orgel.2023.106798.

References

[1] H.W. Kroto, J.R. Heath, S.C. O'Brien, R.F. Curl, R.E. Smalley, C60: buckminsterfullerene, Nature 318 (1985) 162–163.
[2] H.W. Kroto, A.W. Allaf, S.P. Balm, C60 - buckminsterfullerene, Chem. Rev. 91 (1991) 1213–1235.
[3] R.C. Haddon, A.F. Hebard, M.J. Rosseinsky, D.W. Murphy, S.J. Duclos, K.B. Lyons, B. Miller, J.M. Rosamilia, R.M. Fleming, A.R. Kortan, S.H. Glarum, A.V. Makhija, A. J. Muller, R.H. Eick, S.M. Zahurak, R. Tycko, G. Dabbagh, F.A. Thiel, Conducting films of C60 and C70 by alkali-metal doping, Nature 350 (1991) 320–322.
[4] J.-L. Bredas, J.R. Durrant, Organic photovoltaics, Acc. Chem. Res. 42 (2009) 1689–1690.
[5] V.N. Sathiyamoorthy, H. Mizuseki, Y. Kawazoe, Hydrogen storage on nanofullerene cages, Nano 4 (2009) 253–263.
[6] S.S. Han, J.L. Mendoza-Cortés, W.A. Goddard Iii, Recent advances on simulation and theory of hydrogen storage in metal–organic frameworks and covalent organic frameworks, Chem. Soc. Rev. 38 (2009) 1460–1476.
[7] S. Goodarzi, T. Da Ros, J. Conde, F. Sefat, M. Mozafari, Fullerene: biomedical engineers get to revisit an old friend, Mater. Today 20 (2017) 460–480.
[8] J.C. Hummelen, B.W. Knight, F. Lepeq, F. Wudl, J. Yao, C.L. Wilkins, Preparation and characterization of fulleroid and methoanofullerene derivatives, J. Org. Chem. 60 (1995) 532–538.
[9] M.M. Wienk, J.M. Kroon, W.J.H. Verhees, J. Knol, J.C. Hummelen, P.A. van Hal, R. A.J. Janssen, Efficient methano 70 fullerene/MDMO-PPV bulk heterojunction photovoltaic cells, Angew. Chem. Int. Ed. 42 (2003) 3371–3375.
[10] Y. He, H.-Y. Chen, J. Hou, Y. Li, Indene−C60 bisadduct: a new acceptor for high-performance polymer solar cells, J. Am. Chem. Soc. 132 (2010) 1377–1382.
[11] G. Zhao, Y. He, Y. Li, 6.5% efficiency of polymer solar cells based on poly(3-hexylthiophene) and indene-C60 bisadduct by device optimization, Adv. Mater. 22 (2010) 4355–4358.
[12] G. Yu, J. Gao, J.C. Hummelen, F. Wudl, A.J. Heeger, Polymer photovoltacis cells - enhanced efficiencies via a network of internal donor-acceptor heterojunctions, Science 270 (1995) 1789–1791.
[13] M. Bendikov, F. Wudl, D.F. Perepichka, Tetrathiafulvalenes, oligoacenenes, and their buckminsterfullerene derivatives: the brick and mortar of organic electronics, Chem. Rev. 104 (2004) 4891–4946.
[14] B.C. Thompson, J.M.J. Fréchet, Polymer–fullerene composite solar cells, Angew. Chem. Int. Ed. 47 (2008) 58–77.
[15] B. Kippelen, J.-L. Brédas, Organic photovoltaics, Energy Environ. Sci. 2 (2009) 251–261.
[16] S.H. Park, A. Roy, S. Beaupre, S. Cho, N. Coates, J.S. Moon, D. Moses, M. Leclerc, K. Lee, A.J. Heeger, Bulk heterojunction solar cells with internal quantum efficiency approaching 100%, Nat. Photonics 3 (2009) 297–303.
[17] Y.Y. Liang, Z. Xu, J.B. Xia, S.T. Tsai, Y. Wu, G. Li, C. Ray, L.P. Yu, For the bright future-bulk heterojunction polymer solar cells with power conversion efficiency of 7.4%, Adv. Mater. 22 (2010) E135–E138.
[18] M.T. Dang, L. Hirsch, G. Wantz, P3HT:PCBM, best seller in polymer photovoltaic Research, Adv. Mater. 23 (2011) 3597–3602.
[19] Q. Wan, X. Guo, Z. Wang, W. Li, B. Guo, W. Ma, M. Zhang, Y. Li, 10.8% efficiency polymer solar cells based on PTB7-Th and PC71BM via binary solvent additives treatment, Adv. Funct. Mater. 26 (2016) 6635–6640.
[20] H. Yin, H. Lin, Y. Zong, X.-D. Wang, The recent advances in C60 micro/nanostructures and their optoelectronic applications, Org. Electron. 93 (2021), 106142.
[21] J.L. Yang, P. Sullivan, S. Schumann, I. Hancox, T.S. Jones, Organic photovoltaic cells based on unconventional electron donor fullerene and electron acceptor copper hexadecafluorophthalocyanine, Appl. Phys. Lett. 100 (2012), 023307.
[22] Y. Ie, M. Karakawa, S. Jinnai, H. Yoshida, A. Saeki, S. Seki, S. Yamamoto, H. Ohkita, Y. Aso, Electron-donor function of methanofullerenes in donor–acceptor bulk heterojunction systems, Chem. Commun. 50 (2014) 4123–4125.
[23] T. Zhuang, X.-F. Wang, T. Sano, Z. Hong, G. Li, Y. Yang, J. Kido, Fullerene C70 as a P-type donor in organic photovoltaic cells, Appl. Phys. Lett. 105 (2014), 093301.
[24] T.D. Anthopoulos, C. Tanase, S. Setayesh, E.J. Meijer, J.C. Hummelen, P.W. M. Blom, D.M. de Leeuw, Ambipolar organic field-effect transistors based on a solution-processed methanofullerene, Adv. Mater. 16 (2004) 2174–2179.
[25] N.B. Kotadiya, P.W.M. Blom, G.A.H. Wetzelaer, Trap-free space-charge-limited hole transport in a fullerene derivative, Phys. Rev. Appl. 11 (2019), 024069.
[26] N.B. Kotadiya, A. Mondal, P.W.M. Blom, D. Andrienko, G.-J.A.H. Wetzelaer, A window to trap-free charge transport in organic semiconducting thin films, Nat. Mater. 18 (2019) 1182–1186.
[27] G.-J.A.H. Wetzelaer, P.W.M. Blom, Electron and hole transport in solution-processed fullerenes, J. Mater. Chem. C 9 (2021) 16068–16077.
[28] M.J. Frisch, G.W. Trucks, H.B. Schlegel, G.E. Scuseria, M.A. Robb, J.R. Cheeseman, G. Scalmani, V. Barone, G.A. Petersson, H. Nakatsuji, X. Li, M. Caricato, A. V. Marenich, J. Bloino, B.G. Janesko, R. Gomperts, B. Mennucci, H.P. Hratchian, J. V. Ortiz, A.F. Izmaylov, J.L. Sonnenberg, D. Williams-Young, F. Ding, F. Lipparini, F. Egidi, J. Goings, B. Peng, A. Petrone, T. Henderson, D. Ranasinghe, V. G. Zakrzewski, J. Gao, N. Rega, G. Zheng, W. Liang, M. Hada, M. Ehara, K. Toyota, R. Fukuda, J. Hasegawa, M. Ishida, T. Nakajima, Y. Honda, O. Kitao, H. Nakai, T. Vreven, K. Throssell, J.A. Montgomery, J.E. Peralta, F. Ogliaro, M.J. Bearpark, J. J. Heyd, E.N. Brothers, K.N. Kudin, V.N. Staroverov, T.A. Keith, R. Kobayashi, J. Normand, K. Raghavachari, A.P. Rendell, J.C. Burant, S.S. Iyengar, J. Tomasi, M. Cossi, J.M. Millam, M. Klene, C. Adamo, R. Cammi, J.W. Ochterski, R.L. Martin,

K. Morokuma, O. Farkas, J.B. Foresman, D.J. Fox, Gaussian 16, Revision B.01, Gaussian, Inc., Wallingford CT, 2016.
[29] V. Coropceanu, J. Cornil, D.A. da Silva Filho, Y. Olivier, R. Silbey, J.-L. Brédas, Charge transport in organic semiconductors, Chem. Rev. 107 (2007) 926–952.
[30] K.J. Fu, W.L. Karney, O.L. Chapman, S.M. Huang, R.B. Kaner, F. Diederich, K. Holczer, R.L. Whetten, Giant vibrational resonances in A6C60 compounds, Phys. Rev. B 46 (1992) 1937–1940.
[31] E.F. Valeev, V. Coropceanu, D.A. da Silva Filho, S. Salman, J.-L. Brédas, Effect of electronic polarization on charge-transport parameters in molecular organic semiconductors, J. Am. Chem. Soc. 128 (2006) 9882–9886.
[32] Y. Yi, V. Coropceanu, J.-L. Brédas, Nonlocal electron-phonon coupling in the pentacene crystal: beyond the Γ-point approximation, J. Chem. Phys. 137 (2012), 164303.
[33] R.A. Marcus, Electron transfer reactions in chemistry. Theory and experiment, Rev. Mod. Phys. 65 (1993) 599–610.
[34] Y. Yi, V. Coropceanu, J.-L. Brédas, Exciton-dissociation and charge-recombination processes in pentacene/C60 solar cells: theoretical insight into the impact of interface geometry, J. Am. Chem. Soc. 131 (2009) 15777–15783.
[35] R.D. Johnson, G. Meijer, D.S. Bethune, C60 has icosahedral symmetry, J. Am. Chem. Soc. 112 (1990) 8983–8984.
[36] P. Boulas, F. Dsouza, C.C. Henderson, P.A. Cahill, M.T. Jones, K.M. Kadish, Electrochemical properties of C60H2 and C70H21, J. Phys. Chem. 97 (1993) 13435–13437.
[37] W.C. Wan, X. Liu, G.M. Sweeney, W.E. Broderick, Structural evidence for the expected Jahn-Teller distortion in monoanionic C60: synthesis and X-ray crystal structure of decamethylnickelocenium buckminsterfulleride, J. Am. Chem. Soc. 117 (1995) 9580–9581.
[38] M. Perić, L. Andjelković, M. Zlatar, A.S. Nikolić, C. Daul, M. Gruden-Pavlović, Spherical aromaticity of Jahn–teller active fullerene ions, Monatsh. Chem. 144 (2013) 817–823.
[39] C.H. Choi, M. Kertesz, L. Mihaly, Vibrational assignment of all 46 fundamentals of C-60 and C-60(6-): scaled quantum mechanical results performed in redundant internal coordinates and compared to experiments, J. Phys. Chem. A 104 (2000) 102–112.
[40] J.T. Muya, H. Ramanantoanina, C. Daul, M.T. Nguyen, G. Gopakumar, A. Ceulemans, Jahn–teller instability in cationic boron and carbon buckyballs B80 + and C60+: a comparative study, Phys. Chem. Chem. Phys. 15 (2013) 2829–2835.
[41] R.D. Johnson, G. Meijer, J.R. Salem, D.S. Bethune, 2D nuclear-magnetic-resonance study of the structure of the fullerene C70, J. Am. Chem. Soc. 113 (1991) 3619–3621.
[42] G. Sun, M. Kertesz, Vibrational Raman spectra of C70 and C706- studied by density functional theory, J. Phys. Chem. A 106 (2002) 6381–6386.
[43] C. Brink, L.H. Andersen, P. Hvelplund, D. Mathur, J.D. Voldstad, Laser photodetachment of C60− and C70− ions cooled in a storage ring, Chem. Phys. Lett. 233 (1995) 52–56.
[44] M.S. Dresselhaus, G. Dresselhaus, P.C. Eklund, Science of Fullerenes and Carbon Nanotubes, Academic Press, San Diego, CA, 1996.
[45] X.-B. Wang, H.-K. Woo, X. Huang, M.M. Kappes, L.-S. Wang, Direct experimental probe of the on-site coulomb repulsion in the doubly charged fullerene anion C70 2-, Phys. Rev. Lett. 96 (2006), 143002.
[46] C. Boudon, J.P. Gisselbrecht, M. Gross, A. Herrmann, M. Ruttimann, J. Crassous, F. Cardullo, L. Echegoyen, F. Diederich, Redox characteristics of covalent derivatives of the higher fullerenes C70, C76, and C78, J. Am. Chem. Soc. 120 (1998) 7860–7868.
[47] J.A. Mikroyannidis, A.N. Kabanakis, S.S. Sharma, G.D. Sharma, A simple and effective modification of PCBM for use as an electron acceptor in efficient bulk heterojunction solar cells, Adv. Funct. Mater. 21 (2011) 746–755.
[48] P. Morvillo, E. Bobeico, Bisadducts of C70 as electron acceptors for bulk heterojunction solar cells: a theoretical study, Fullerenes, Nanotub. Carbon Nanostruct. 19 (2011) 410–420.
[49] A.M. Nardes, A.J. Ferguson, J.B. Whitaker, B.W. Larson, R.E. Larsen, K. Maturová, P.A. Graf, O.V. Boltalina, S.H. Strauss, N. Kopidakis, Beyond PCBM: understanding the photovoltaic performance of blends of indene-C60 multiadducts with poly(3-hexylthiophene), Adv. Funct. Mater. 22 (2012) 4115–4127.
[50] B.W. Larson, J.B. Whitaker, X.-B. Wang, A.A. Popov, G. Rumbles, N. Kopidakis, S. H. Strauss, O.V. Boltalina, Electron affinity of phenyl–C61–butyric acid methyl ester (PCBM), J. Phys. Chem. C 117 (2013) 14958–14964.
[51] E.T. Hoke, I.T. Sachs-Quintana, M.T. Lloyd, I. Kauvar, W.R. Mateker, A.M. Nardes, C.H. Peters, N. Kopidakis, M.D. McGehee, The role of electron affinity in determining whether fullerenes catalyze or inhibit photooxidation of polymers for solar cells, Adv. Energy Mater. 2 (2012) 1351–1357.
[52] K. Akaike, K. Kanai, H. Yoshida, J.y. Tsutsumi, T. Nishi, N. Sato, Y. Ouchi, K. Seki, Ultraviolet photoelectron spectroscopy and inverse photoemission spectroscopy of [6,6]-Phenyl-C61-butyric acid methyl ester in gas and solid phases, J. Appl. Phys. 104 (2008), 023710.
[53] O.V. Boltalina, I.N. Ioffe, L.N. Sidorov, G. Seifert, K. Vietze, Ionization energy of fullerenes, J. Am. Chem. Soc. 122 (2000) 9745–9749.
[54] H. Yu, H.-H. Cho, C.-H. Cho, K.-H. Kim, D.Y. Kim, B.J. Kim, J.H. Oh, Polarity and air-stability transitions in field-effect transistors based on fullerenes with different solubilizing groups, ACS Appl. Mater. Interfaces 5 (2013) 4865–4871.
[55] H. Sun, S. Ryno, C. Zhong, M.K. Ravva, Z. Sun, T. Körzdörfer, J.-L. Brédas, Ionization energies, electron affinities, and polarization energies of organic molecular crystals: quantitative estimations from a polarizable continuum model (PCM)-Tuned range-separated density functional approach, J. Chem. Theor. Comput. 12 (2016) 2906–2916.
[56] N. Sato, Y. Saito, H. Shinohara, Threshold ionization energy of C60 in the solid state, Chem. Phys. 162 (1992) 433–438.
[57] A. Nogimura, K. Akaike, R. Nakanishi, R. Eguchi, K. Kanai, Electronic structure and surface morphology of [6,6]-phenyl-C71-butyric acid methyl ester films, Org. Electron. 14 (2013) 3222–3227.
[58] Y. Park, V. Choong, Y. Gao, B.R. Hsieh, C.W. Tang, Work function of indium tin oxide transparent conductor measured by photoelectron spectroscopy, Appl. Phys. Lett. 68 (1996) 2699–2701.
[59] Y. Qi, S.K. Mohapatra, S. Bok Kim, S. Barlow, S.R. Marder, A. Kahn, Solution doping of organic semiconductors using air-stable N-dopants, Appl. Phys. Lett. 100 (2012), 083305.
[60] J. Nelson, J.J. Kwiatkowski, J. Kirkpatrick, J.M. Frost, Modeling charge transport in organic photovoltaic materials, Acc. Chem. Res. 42 (2009) 1768–1778.
[61] D.L. Cheung, A. Troisi, Theoretical study of the organic photovoltaic electron acceptor PCBM: morphology, electronic structure, and charge localization, J. Phys. Chem. C 114 (2010) 20479–20488.
[62] V.P. Antropov, O. Gunnarsson, A.I. Liechtenstein, Phonons, electron-phonon, and electron-plasmon couplings in C60 compounds, Phys. Rev. B 48 (1993) 7651–7664.
[63] O. Gunnarsson, H. Handschuh, P.S. Bechthold, B. Kessler, G. Gantefor, W. Eberhardt, Photoemission spectra of C60(-) - electron-phonon coupling, Jahn-Teller effect, and superconductivity in the fullerides, Phys. Rev. Lett. 74 (1995) 1875–1878.
[64] N. Iwahara, T. Sato, K. Tanaka, L.F. Chibotaru, Vibronic coupling in C60- anion revisited: derivations from photoelectron spectra and DFT calculations, Phys. Rev. B 82 (2010), 245409.
[65] N.R. Tummala, Z. Zheng, S.G. Aziz, V. Coropceanu, J.-L. Brédas, Static and dynamic energetic disorders in the C60, PC61BM, C70, and PC71BM fullerenes, J. Phys. Chem. Lett. 6 (2015) 3657–3662.
[66] N.R. Tummala, S.A. Elroby, S.G. Aziz, C. Risko, V. Coropceanu, J.-L. Brédas, Packing and disorder in substituted fullerenes, J. Phys. Chem. C 120 (2016) 17242–17250.
[67] D.L. Dorset, M.P. McCourt, Disorder and the molecular packing of C60 buckminsterfullerene: a direct electron-crystallographic analysis, Acta Crystallogr. A 50 (1994) 344–351.
[68] M. Casalegno, S. Zanardi, F. Frigerio, R. Po, C. Carbonera, G. Marra, T. Nicolini, G. Raos, S.V. Meille, Solvent-free phenyl-C61-butyric acid methyl ester (PCBM) from clathrates: insights for organic photovoltaics from crystal structures and molecular dynamics, Chem. Commun. 49 (2013) 4525–4527.
[69] F. Zhao, X. Meng, Y. Feng, Z. Jin, Q. Zhou, H. Li, L. Jiang, J. Wang, Y. Li, C. Wang, Single crystalline indene-C60 bisadduct: isolation and application in polymer solar cells, J. Mater. Chem. 3 (2015) 14991–14995.
[70] S. Rossbauer, C. Müller, T.D. Anthopoulos, Comparative study of the N-type doping efficiency in solution-processed fullerenes and fullerene derivatives, Adv. Funct. Mater. 24 (2014) 7116–7124.